Chemical Engineering Journal 431 (2022) 134095

Contents lists available at ScienceDirect

Chemical Engineering Journal

journal homepage: www.elsevier.com/locate/cej

New insights into glyphosate adsorption on modified carbon nanotubes via green synthesis: Statistical physical modeling and steric and energetic interpretations

Júlia C. Diel [a], Kátia da Boit Martinello [b], Christian L. da Silveira [a], Hércules A. Pereira [c], Dison S. P. Franco [a], Luis F.O. Silva [d], Guilherme L. Dotto [a,b,*]

[a] Chemical Engineering Department, Federal University of Santa Maria, 97105-900 Santa Maria, Brazil
[b] Department of Health Sciences, Universidad de la Costa, CUC, Calle 58 # 55–66, Barranquilla, Atlántico, Colombia
[c] Chemistry Department, Federal University of Santa Maria, 97105-900 Santa Maria, Brazil
[d] Department of Civil and Environmental, Universidad de la Costa, CUC, Calle 58 # 55–66, Barranquilla, Atlántico, Colombia

ARTICLE INFO

Keywords:
Glyphosate
Carbon nanotubes
Green synthesis
Adsorption isotherms
Statistical physics
Adsorption mechanism

ABSTRACT

The present work used a statistical physics approach to present new insights into the adsorption of the pesticide glyphosate on modified carbon nanotubes via green synthesis (MWCNT/MPNs-Fe). The experimental equilibrium curves obtained for this system under pH 4 at temperatures 298, 308, 318, and 328 K were simulated from monolayer, double layer, and multilayer models, with 1 and 2 energies, considering real and ideal fluid approaches. Taking into account the statistical indicators and the physical meaning of the parameters, exploring simplifying hypotheses, the Hill model with 1 energy and ideal fluid approach (M1) presented the best prediction of the experimental data, indicating that glyphosate adsorption occurs by the formation of a monolayer and that pesticide interaction with MWCNT/MPNs-Fe are characterized by only one energy. Based on this approach, to assess the steric aspects of the system, the number of molecules adsorbed per site (n), the density of receptor sites (N_m), adsorption capacity at saturation (Q_{sat}), and concentration at half-saturation (W) were interpreted. As for the energetic aspects, the adsorption energy (ΔE) was inferred. The combination of parameters to its evolution with temperature and the magnitude of ΔE indicated an exothermic process involving a physical interaction mechanism. Finally, the new insights showed that the MWCNT/MPNs-Fe adsorbent favored pesticide adsorption by interacting glyphosate molecules with the metallic iron nanoparticles present on the adsorbent surface.

1. Introduction

Emerging contaminants (ECs) are a group of substances, such as pesticides, dyes, metals, pharmaceuticals, and personal care products, which have been frequently detected in wastewater, surface, and groundwater, usually from inadequate agricultural and industrial discharges [1]. The emerging character implies contaminants recently added to the environment and the awareness and concern that their negative impacts are causing in international communities [2]. Specifically, about pesticides, glyphosate (GLY) (Fig. 1) is a synthetic, non-selective, and widely applicable compound [3], which stands out as the most used and marketed pesticide in the world for the control of weeds and invasive species to the plantation [4]. However, after application, the total concentration of GLY in soil and water can vary, suffering natural decomposition in the period between 1 and 26 weeks, becoming a resistant contaminant, and posing risks to fauna and flora [5,6]. Moreover, exposure to GLY and its residues/by-products is considered toxicologically harmful even at low concentrations. It can cause cardiac, respiratory, and neurological problems and be associated with carcinogenic, mutagenic, and genotoxic effects [7].

Several technologies are developed and applied to promote the removal of ECs from water resources, such as membrane separation methods [8], electrolysis [9], photocatalytic degradation [10], advanced oxidative processes [11], microwave radiation [12], ozonation [13], and ultraviolet irradiation [6]. However, most of these remediation technologies have limited flexibility, high cost, low efficiency, and possible production of secondary pollutants [14]. In this sense, adsorption is a promising technique, characterized by low cost,

* Corresponding author.
E-mail address: guilherme.dotto@ufsm.br (G.L. Dotto).

https://doi.org/10.1016/j.cej.2021.134095
Received 23 September 2021; Received in revised form 6 December 2021; Accepted 8 December 2021
Available online 13 December 2021

design simplicity, ease of operation, and high efficiency [15,16], avoiding secondary pollution and allowing the use of numerous materials as adsorbents [17]. In addition, it presents adsorbents regeneration and reuse capacity, enabling the process in the long term [18]. Among the adsorbents already used as efficient alternatives for GLY removal, the following can be reported: chitosan biopolymer membrane [19], D301 resin [20], rice husk biochar [21], graphene oxide functionalized with $MnFe_2O_4$ [22], wood biochar [23], activated tannery sludge [24], zeolite 4A [25] and amine-functionalized star-shaped polymeric particles [26].

Recently, with the advances in nanotechnology, carbon nanotubes (CNTs) have emerged as promising adsorbents, especially multi-walled carbon nanotubes (MWCNTs), due to their properties, such as a high specific surface area with high molecular capture capacity of pollutants, porous and layered structure [27,28]. The use of CNTs has already been proposed in the adsorption of drugs [29,30], dyes [31,32], metal ions [33,34], formic acid [35], phenolic compounds [36], and sulfur dioxide [37]. However, the CNT's adsorption properties are often impaired, depending on the contaminant. It is necessary to improve their potential by increasing their selectivity and adsorptive capacity by adding functional groups, such as OH and COOH, and modifying their surface [38]. In the case of GLY, the modification of CNTs by impregnating metallic nanoparticles (MNPs) through a green synthesis route proved to be a viable alternative to increase the intensity of interaction with the surface of the adsorbent introducing adsorption sites [39].

Regardless of the adsorbent adopted and the contaminant in question, it is essential to determine the interactions that occur at the solid/liquid interface, which depend on the characteristics of the adsorbent, the adsorbate, and the solution. The interpretation of process equilibrium through the construction and modeling of adsorption isotherms is a way to infer interactions between adsorbate-adsorbent [27]. In modeling, adsorption processes are generally elucidated by applying Langmuir, Freundlich, and Sips models. Although these models are easy to describe from the experimental data, the information provided may be limited or incomplete, as they do not have a physical meaning or relationship with the physicochemical parameters of the adsorbent and the adsorbate [40]. Thus, integrating experimental results with physical-statistical models enables a detailed and reliable description of the process. Statistical physics models correlate the adsorbate molecules with the macroscopic properties of the adsorbent materials, providing steric and energetic information about the adsorptive process [41,42]. These models' parameters include the number of molecules adsorbed per site, the density of receptor sites, the amount adsorbed in saturation, the total number of formed layers, the concentration at half-saturation, and the adsorption energy [43]. The interpretation of physical-statistical parameters can help new works, instigating the preparation and optimization of novel materials and the adsorptive process.

The authors carried out previous studies aiming to modify MWCNTs via green synthesis, the characterization of the synthesized material, and the performance of adsorption tests for the removal of GLY in the aqueous matrix [39]. However, so far, there are no reports of analysis and modeling of the adsorption of this herbicide from the perspective of statistical physics. In this sense, the present contribution provided new insights into the equilibrium data obtained in Diel et al. [44] for temperatures ranging from 298 to 328 K (pH = 4). For this, six models based on statistical physics were applied: Hill model with 1 energy for ideal fluid, Hill model with 2 energies for ideal fluid, Hill model with 1 energy for real fluid, Hill model with 2 energies for real fluid, double layer model with two energy, and multilayer model. Based on the simulation data obtained, the best fit model was selected to interpret the steric and energetic parameters, evaluating the possible adsorption mechanisms associated with the GLY and the adsorbent used.

2. Description of experimental data

2.1. Adsorbent and adsorbate

Multi-walled carbon nanotubes functionalized with COOH groups (purity: 95%, COOH content: 1.47–1.63% mass fraction) were purchased from Nanostructure & Amorphous Materials, Inc. (USA). These commercial nanotubes supported the impregnation of metallic iron nanoparticles (MPNs-Fe) via green synthesis methodology. Nutshells (*Carya illinoinensis*) were used as a natural reducing agent, and iron sulfate ($FeSO_4{\cdot}7H_2O$, CAS: 7782–63-0, 99.99%, Neon) was used as a metal salt for reduction. The preparation and characterization of the modified material, labeled MWCNT/MPNs-Fe, were described in detail in the reported reference [39,44].

The modified material MWCNT/MPNs-Fe was used as an adsorbent in the removal of GLY ($C_3H_8NO_5P$, molecular weight: 169.073 g mol^{-1}, CAS: 1071–83-6, purity: 98%, Sigma-Aldrich) in the aqueous matrix and the adsorption results obtained (pH study, kinetic and equilibrium modeling, thermodynamic behavior, simulated effluent, and material regeneration) are included in the same reference [39,44]. Ninhydrin ($C_9H_6O_4$, CAS: 485–47-2, Sigma-Aldrich) and sodium molybdate ($MoNa_2O_4$, CAS: 7631–95-0, purity: 98%, Sigma-Aldrich) were used for colorimetric complexation reaction [45], allowing the quantification of the pesticide in a UV–Vis spectrophotometer (Shimadzu, model: UV-2600, Japan), at 570 nm.

2.2. Adsorption isotherms

GLY adsorption isotherms using MWCNT/MPNs-Fe were experimentally determined at 298, 308, 318, and 328 K in a thermostatic stirrer (Solab, SL-222, Brazil). The experimental conditions were:

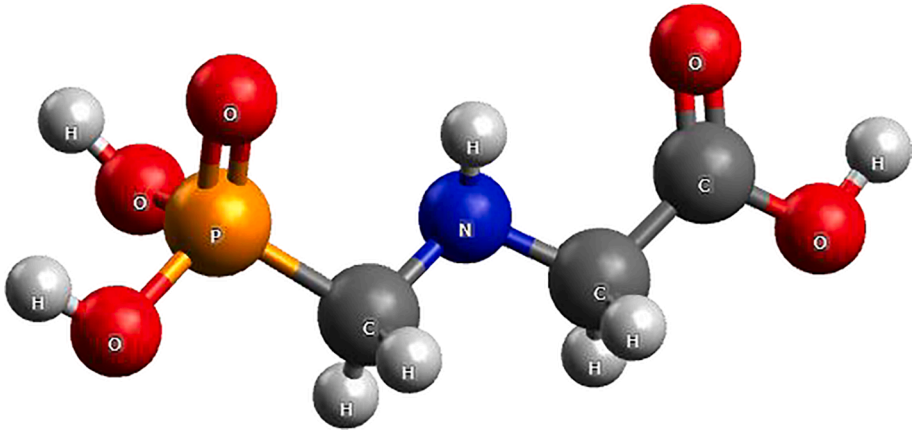

Fig. 1. Molecular structure of the GLY herbicide.

agitation rate of 160 rpm, solution pH equal to 4, the adsorbent dosage of 1.5 g L^{-1}, and initial GLY concentrations ranging from 0 to 150 mg L^{-1}. The adsorbent was inserted into the GLY solutions, and all suspensions were stirred until reaching adsorption equilibrium (240 min of contact). Then, the liquid phase was separated from the solid by filtration, and the samples were submitted to colorimetric complexation methodology by adding ninhydrin and sodium molybdate. The remaining GLY concentrations were quantified. The tests were carried out in triplicate. The equilibrium adsorption capacity (Q_e, mg g^{-1}) was determined using Equation (1):

$$Q_e = \frac{V\,(\,C_0\,-\,C_e\,)}{m} \tag{1}$$

Where C_0 (mg L^{-1}) is the initial concentration of GLY in the liquid phase; C_e (mg L^{-1}) is the concentration of GLY in the liquid phase measured at equilibrium; V (L) is the volume of the solution, and m (g) is the mass of adsorbent used.

3. Description of statistical physics models

The experimental equilibrium data were used to carry out the theoretical study of the GLY adsorption mechanism on MWCNT/MPNs-Fe. For this study, six models based on the formalism of the theory of statistical physics were selected to simulate the adsorption isotherms at different temperatures: Hill model with 1 energy for ideal fluid (M1), Hill model with 2 energies for ideal fluid (M2), Hill model with 1 energy for real fluid (M3), Hill model with 2 energies for real fluid (M4), double layer model with 2 energies (M5), and multilayer model (M6). These models are presented in detail in the next subsections.

The descriptions show that isotherms can be simulated by monolayer, double layer, or multilayer models, considering the ideal gas law and real gas law approaches [46]. All models were developed from the canonical grand set partition function. The partition function (z_{gc}), expressed by Equation (2), describes the microscopic states of an adsorption system depending on the physical condition to which the system is subject [18,47].

$$z_{gc} = \sum_{N_i=0,\ 1,\ 2\ldots}^{\infty} e^{-\beta(\varepsilon-\mu)N_i} \tag{2}$$

Where ε (kJ mol^{-1}) represents the adsorption energy of the receiving site; μ (kJ mol^{-1}) is the chemical potential of this receptor site; N_i is the occupied state of the receiving site (equivalent to 0 if the site is empty, and equal to 1 if the site is occupied); β represents the Boltzmann factor, defined as $1/(k_BT)$, k_B is the Boltzmann constant (13806488×10^{-23} J K^{-1}) and T the temperature (K).

The choice of the tested models was based on the physicochemical characteristics of the system, considering two types of adsorption sites available in MWCNTs (the MPNs-Fe and the COOH functional group) and two types of interaction with different energies (interaction of the GLY molecule with the MPNs-Fe and interaction of the GLY molecule with the COOH functional group). Consequently, for the development of the selected models, some hypotheses were considered, facilitating the interpretations. As a first approximation, the GLY molecules were treated as an ideal gas, disregarding the mutual interaction between them since their concentration is evaluated as relatively low [27,42]. Another assumption considered real situations in which the intermolecular interactions between GLY molecules were not neglected. As the last approach, the internal energies of the GLY molecules (rotational, vibrational, and electronic) were neglected as they are insignificant compared to the translational energies [48].

The Lennard-Jones expression (Equation (3)) was applied to consider the potential energies of interaction between GLY molecules [49].

$$U(r) = u_0\left(\left(\frac{r_0}{r}\right)^{12} - 2\left(\frac{r_0}{r}\right)^{6}\right) \tag{3}$$

Where r equals the distance between the centers of two neighboring molecules; r_0 represents the minimum potential energy distance between two molecules, and u_0 is the potential for interaction between the adsorbate molecules.

For models considering real fluid, non-ideality was represented by the Van der Waals equation of state (VDW) (Equation (4)) [49].

$$\left(P + \frac{aN^2}{V^2}\right)(V - Nb) = Nk_BT \tag{4}$$

Where P (Pa) represents the pressure; V (m^3) is the volume; T (K) is the temperature; N is the number of molecules; a (J L mg^{-1}) and b (L mg^{-1}) represent the VDW parameters of cohesion pressure and covolume of the adsorbate molecule, defined by Equations (5) and (6), respectively.

$$\frac{a}{N_A} = \frac{5}{3}u_0\frac{2}{3}\pi r_0^3 \tag{5}$$

$$\frac{b}{N_A} = \frac{2}{3}\pi r_0^3 \tag{6}$$

where $N_A = 6.0221409 \times 10^{23}$ molecules mol^{-1}, is the Avogadro number

3.1. Hill model with 1 energy for ideal fluid (M1)

The first model assumes that GLY adsorption occurs through the formation of a monolayer, that is, a single layer of molecules on the surface of the adsorbent [15,42]. This model also hypothesizes that the pesticide interactions with MWCNT/MPNs-Fe are characterized by only one energy (ΔE, kJ mol^{-1}), constant for all active sites involved in adsorption [40]. Furthermore, it is assumed that the leading adsorption site can capture a variable number of GLY molecules defined by the parameter n [50]. For M1, the variation of the adsorbed amount (Q_a, mg g^{-1}) as a function of the equilibrium concentration (C, mg L^{-1}) is provided by Equation (7).

$$Q_a = \frac{nN_m}{1 + \left(\frac{W}{C}\right)^n} \tag{7}$$

Where the parameter n (dimensionless) represents the number of pesticide molecules captured per active site of the adsorbent; N_m (mg g^{-1}) describes the density of active receptor sites, and W (mg L^{-1}) indicates the concentration at half-saturation. When the material has more than one adsorption site, different values of n referring to the available sites are estimated.

3.2. Hill model with 2 energies for ideal fluid (M2)

This model also assumes that GLY adsorption occurs through the formation of a monolayer but assumes that the pesticide molecules are adsorbed on two different adsorption sites on the adsorbent (MPNs-Fe and COOH functional group) with two different energy levels (ΔE_1 for the first site and ΔE_2 for the second, kJ mol^{-1}). Thus, the leading adsorption site can capture a variable number of molecules indicated by n_1 and n_2 [50,51]. The variation of the adsorbed amount as a function of the equilibrium concentration for M2 is given by Equation (8).

$$Q_a = \frac{n_1N_{1m}}{1 + \left(\frac{W_1}{C}\right)^{n_1}} + \frac{n_2N_{2m}}{1 + \left(\frac{W_2}{C}\right)^{n_2}} \tag{8}$$

Where N_{1m} and N_{2m} (mg g^{-1}) are the densities of the first and second receiving site, respectively, and W_1 and W_2 (mg L^{-1}) are the concentrations at half-saturation for the first and second receptor site, respectively. Subscript 1 represents the adsorption site of the MNPs-Fe, and subscript 2 is the adsorption site of the COOH group.

3.3. Hill model with 1 energy for real fluid (M3)

This model considers the assumptions of the M1 model (monolayer formation, interactions characterized by energy) but assumes that the intermolecular interactions between GLY molecules cannot be neglected. It uses the Van der Waals equation of state and its parameters to build this model [27,49]. The expression for applying M3 is given by Equation (9).

$$Q_a = \frac{nN_m}{1 + \left(\frac{W}{C}(1 - bC)e^{2\beta aC}e^{\frac{-bC}{1-bC}}\right)^n} \tag{9}$$

3.4. Hill model with 2 energies for real fluid (M4)

Likewise, this model considers the assumptions of the M2 model (monolayer formation, with molecules, adsorbed at two different adsorption sites with different energy levels), assuming that the intermolecular interactions between the GLY molecules cannot be ignored [27,49]. The mathematical formulation of M4 is expressed by Equation (10).

$$Q_a = \frac{n_1N_{1m}}{1 + \left(\frac{W_1}{C}(1 - bC)e^{2\beta aC}e^{\frac{-bC}{1-bC}}\right)^{n_1}} + \frac{n_2N_{2m}}{1 + \left(\frac{W_2}{C}(1 - bC)e^{2\beta aC}e^{\frac{-bC}{1-bC}}\right)^{n_2}} \tag{10}$$

3.5. Double-layer model with 2 energies (M5)

This model was formulated considering that the removal of GLY involves a double layer adsorption process; that is, two layers of adsorbate were formed on the surface of MWCNT/MPNs-Fe [15]. In this case, the adsorption is hypothesized by forming two adsorbed layers of GLY but characterized by two different types of interactions for these layers. First, adsorbate-adsorbent and adsorbate–adsorbate interactions are considered [40]. Second, it is assumed that the first adsorbed layer has an adsorption energy level ΔE_1 (kJ mol^{-1}). In contrast, the second layer has a different adsorption energy level ΔE_2 (kJ mol^{-1}), which is supposed to be less than the first since the first molecules are adsorbed directly on the surface and therefore have higher energy [43,46]. And for the occupation status Ni, it is assigned a value of 0 if the site is empty, a value of 1 if n molecules occupy the site, and 2n if the site is occupied by two molecules [51]. The mathematical expression of M5 is defined by Equation (11).

$$Q_a = \frac{nN_m\left(\frac{C}{W_1}\right)^n + 2\left(\frac{C}{W_2}\right)^{2n}}{1 + \left(\frac{C}{W_1}\right)^n + \left(\frac{C}{W_2}\right)^{2n}} \tag{11}$$

W_1 and W_2 (mg L^{-1}) are the concentrations at half-saturation related to the first and second layers formed, respectively.

3.6. Multilayer model (M6)

Finally, the last model tested to analyze GLY adsorption assumes the presence of a multilayer process. It assumes the formation of a variable but a limited number of adsorbate layers [52]. In this sense, this model was applied to estimate approximately the total number of layers formed, represented by the parameter $(1 + N_2)$ [43]. In the M7 formulation, the multilayer adsorption considers two energies: the molecules of the first layer interact with the surface of the material being adsorbed with energy ΔE_1 (kJ mol^{-1}), and the molecules of the other layers N_2 are adsorbed with energy ΔE_2 (kJ mol^{-1}) [42,43,51]. The expression of the M7 multilayer adsorption model is given by Equation (12).

$$Q_a = \frac{nN_m[F_1(C) + F_2(C) + F_3(C) + F_4(C)]}{[G(C)]} \tag{12}$$

$$F_1(C) = \frac{-2\left(\frac{C}{W_1}\right)^{2n}}{1 - \left(\frac{C}{W_1}\right)^n} + \frac{\left(\frac{C}{W_1}\right)^n\left(1 - \left(\frac{C}{W_1}\right)^{2n}\right)}{\left(1 - \left(\frac{C}{W_1}\right)^n\right)^2} \tag{13}$$

$$F_2(C) = \frac{2\left(\frac{C}{W_1}\right)^n\left(\frac{C}{W_2}\right)^n\left(1 - \left(\frac{C}{W_2}\right)^{nN_2}\right)}{1 - \left(\frac{C}{W_2}\right)^n} \tag{14}$$

$$F_3(C) = \frac{-N_2\left(\frac{C}{W_1}\right)^n\left(\frac{C}{W_2}\right)^n\left(\frac{C}{W_2}\right)^{nN_2}}{1 - \left(\frac{C}{W_2}\right)^n} \tag{15}$$

$$F_4(C) = \frac{\left(\frac{C}{W_1}\right)^n\left(\frac{C}{W_2}\right)^{2n}\left(1 - \left(\frac{C}{W_2}\right)^{nN_2}\right)}{\left(1 - \left(\frac{C}{W_2}\right)^n\right)^2} \tag{16}$$

$$G(C) = \frac{\left(1 - \left(\frac{C}{W_1}\right)^{2n}\right)}{1 - \left(\frac{C}{W_1}\right)^n} + \frac{\left(\frac{C}{W_1}\right)^n\left(\frac{C}{W_2}\right)^n\left(1 - \left(\frac{C}{W_2}\right)^{nN_2}\right)}{1 - \left(\frac{C}{W_2}\right)^n} \tag{17}$$

Where W_1 and W_2 (mg L^{-1}) are the concentrations at half-saturation of the first and other formed layers, respectively, and N_2 (dimensionless) represents the number of layers formed.

4. Adjusting the data and selecting the appropriate model

Statistical physical modeling of experimental GLY adsorption data and parameter estimation of the models described in Section 3 were performed using two combined numerical techniques.

The models have parameters that not only have different magnitudes. At the same time, the density of the receptor active sites (Nm) value is in the order of tens. The cohesion pressure parameters (a) are much smaller than that; for this reason, the search region for the optimal parameters is very broad. The objective function to be minimized may contain local minima. To avoid local minima convergence, we used a Particle Swarm Optimization algorithm (PSO, particleswarm function of MATLAB software) [53,54] to initially search for the most promising region for the global minimum of the Least Squares Objective Function. After obtaining a solution using the particleswarm algorithm, the results were assumed as initial guesses for a Levenberg-Marquardt algorithm (lsqnonlin function of MATLAB software) [55–57] as a form of final refinement of the obtained solution [58,59].

The goodness of fit was statistically assessed using the coefficient of determination (R^2), the root means square error (RMSE), and the Akaike information criterion (AIC), as detailed in the Supplementary Material.

5. Results and discussion

5.1. Model selection and estimated parameters

All the models described were fitted to the experimental data of the isothermal adsorption curves at different temperatures (298, 308, 318, and 328 K). The selection of the best model for the interpretation of GLY adsorption in MWCNT/MPNs-Fe was based, firstly, on the statistical indicators R^2, RMSE, and AIC, whose values obtained are listed in Tables 1, 2, and 3, respectively.

According to the results reported in Tables 1, 2, and 3, it is seen that the M5 model presented the least satisfactory correlation at all study temperatures, with the R^2 varying from 0.8379 to 0.9511, the RMSE

Table 1
Values of determination coefficient (R^2) of each adsorption model at different temperatures.

Model	298 K	308 K	318 K	328 K
Hill with one energy (ideal fluid) (M1)	0.9967	0.9925	0.9878	0.9910
Hill with two energies (ideal fluid) (M2)	0.9980	0.9999	0.9999	0.9966
Hill with one energy (real fluid) (M3)	0.9965	0.9915	0.9861	0.9898
Hill with two energies (real fluid) (M4)	0.9653	0.9964	0.9969	0.9849
Double layer with two energies (M5)	0.9511	0.8379	0.8845	0.8394
Multilayer (M6)	0.9977	0.9999	0.9881	0.9916

Table 2
Values of each adsorption model's root of mean square error (RMSE) at different temperatures.

Model	298 K	308 K	318 K	328 K
Hill with one energy (ideal fluid) (M1)	0.1808	0.2693	0.3193	0.2445
Hill with two energies (ideal fluid) (M2)	0.1396	0.0232	0.0005	0.1498
Hill with one energy (real fluid) (M3)	0.1867	0.2867	0.3400	0.2603
Hill with two energies (real fluid) (M4)	0.5836	0.1858	0.1611	0.3172
Double layer with two energies (M5)	0.6932	1.2516	0.9811	1.0331
Multilayer (M6)	0.1512	0.0313	0.3146	0.2365

Table 3
Values of Akaike information criterion (AIC) of each adsorption model at different temperatures.

Model	298 K	308 K	318 K	328 K
Hill with one energy (ideal fluid) (M1)	−64.17	−48.22	−41.41	−52.09
Hill with two energies (ideal fluid) (M2)	−67.44	−139.27	−294.14	−64.62
Hill with one energy (real fluid) (M3)	−58.60	−41.44	−34.63	−45.31
Hill with two energies (real fluid) (M4)	−2.67	−48.45	−54.16	−27.06
Double layer with two energies (M5)	−8.46	15.18	5.44	7.51
Multilayer (M6)	−67.03	−130.08	−37.73	−49.14

from 0.6932 to 1.2516, and the AIC from −8.46 to 15.18. In sequence, the M4 model presented a good fit to the data, but with greater instability to temperature, varying the R^2 from 0.9653 to 0.9969, the RMSE from 0.1611 to 0.5836, and the AIC from −54.16 to −2.67. Consequently, the double layer model with 2 energies (M5) and the Hill model with 2 energies and real fluid approach (M4) were discarded, considering that they are inadequate to interpret the isotherms.

Concerning models M1, M2, M3, and M6, the values of R^2 were very close to unity, indicating a satisfactory correlation between the experimental data and the values estimated by the models. As the difference between the coefficient of determination values was not significant ($0.9861 < R^2 < 0.9999$), this observation suggests that both models (M1, M2, M3, and M6) could be used to interpret the GLY adsorption mechanism. However, as already stated by Sellaoui et al. [60] and Toumi et al. [47], the selection criteria for the best model are not limited only to statistical indicators; they are also based on the physical meaning of the parameters obtained. In this sense, a detailed analysis of the evolution of the parameters as a function of temperature indicated that models M2 and M6 presented some inconsistencies. In the M6 multilayer model, the parameter N_2 considers different scenarios of the adsorption mechanism, assuming the formation of a fixed number of layers of pesticide molecules (0, 1, 2, 3, 4, etc.) [61]. When simulating the data through this model, establishing an adjustable upper limit for estimating N_2 (0, 1, or 2, for example, assuming monolayer, double or triple layer), this parameter always ends up reaching the threshold value, no variations as a function of temperature. And without setting limits, the values obtained for N_2 do not coincide with a real number of layers, having no physical meaning. Thus, although some authors point out that the description of the phenomenon is better due to the greater number of parameters [43], M6 model is not applicable. The same happens with the M2 monolayer model: by adjusting the combination of lower and upper limits for parameter estimation, all parameters with physical meaning are not reached, making an adequate assessment impossible, although the indicators point to quality in the adjustment. Consequently, the M2 and M6 models were also discarded to interpret the adsorption mechanism, and, finally, the selection was limited to the M1 and M3 models.

Thus, from the initial information regarding the discarded models, it can be inferred that the adsorption of GLY in MWCNT/MNPs-Fe does not form a double layer (M5) or multilayers (M6). Furthermore, considering that the models with 2 energies were disregarded (M2 and M4), it appears that the pesticide interactions with MWCNT/MPNs-Fe are characterized by only one energy, constant for all active sites involved in adsorption.

Therefore, Hill models with 1 energy and ideal fluid approach (M1) and Hill model with 1 energy and real fluid approach (M3) were initially selected to interpret the adsorption isotherms of GLY on MWCNT/MNPs-Fe. This selection means that choosing a single fixed model is not spontaneous, and parameter values do not differ significantly between models [62]. The estimated values for model parameters M1 (n, N_m, W) and M3 (n, N_m, W, a, b) are summarized in Tables 4 and 5, respectively. These parameters allowed the determination of the saturation adsorption capacity (Q_{sat}, mg g^{-1}) from Equation (18) and the adsorption energy (ΔE, kJ mol^{-1}) from Equation (19).

$$Q_{sat} = nN_m \tag{18}$$

$$\Delta E = RT\ ln\left(\frac{Cs}{W}\right) \tag{19}$$

Where R is the ideal gas constant (8,31446 J mol^{-1} K^{-1}; and Cs is the solubility of GLY in water (12 g L^{-1}) [63], assumed to be constant at all temperatures to simplify interpretation.

Fig. 2 represents the adsorption equilibrium curves (experimental and modeled) at different temperatures. In (a), the curves are fitted to the M1 model and (b) to the M3 model. The solid black lines prove that both models could predict the experimental data with great accuracy.

Diel et al. [44] classified the experimental curves in Fig. 2 as having a typical L2 isotherm shape associated with favorable adsorption. The "L" class considers that higher concentrations of adsorbate in solution gradually lead to an increase in the adsorption capacity until the saturation of the sites available in the adsorbent particles, with the maximum capacity being detected by the achievement of a plateau in the isotherm, as indicated by the subclass " two" [64,65]. In addition, a tendency to reduce the adsorptive amount with increasing temperature was identified, which corresponds to an exothermic adsorption process in this temperature range. This adsorption behavior can be evaluated by statistical physics to obtain interpretations at the molecular level.

Since the estimated parameters for the M1 and M3 models were very close, some authors point out that the adsorption phenomenon is better described when a maximum of physical magnitudes are included [66]; the description of the phenomenon is better from the M1 model. According to Occam's razor theory, one should always choose the simplest model among two models with the same performance since the simplest

Table 4
Values of the physical-statistical parameters considering the M1 model for the GLY adsorption system on MWCNT/MPNs-Fe.

Parameters of M1 model	Temperature (K)			
	298	308	318	328
n	0.67	1.56	1.32	1.66
N_m	65.03	22.56	25.80	18.20
W (mg L^{-1})	6.02	7.17	8.42	10.16
Q_{sat} (mg g^{-1})	43.66	35.12	34.03	30.22
ΔE (kJ mol^{-1})	−18.82	−19.01	−19.20	−19.29

Table 5
Values of the physical-statistical parameters considering the M3 model for the GLY adsorption system on MWCNT/MPNs-Fe.

Parameters of M3 model	Temperature (K)			
	298	308	318	328
n	0.72	1.56	1.32	1.66
N_m	54.13	22.56	25.80	18.21
W (mg L^{-1})	4.55	7.17	8.42	10.16
a (J L mg^{-1})	$1x10^{-65}$	$1x10^{-65}$	$1x10^{-65}$	$1x10^{-65}$
b (L mg^{-1})	0.0056	$1x10^{-14}$	$1x10^{-14}$	$1x10^{-14}$
Q_{sat} (mg g^{-1})	38.89	35.12	34.03	30.22
ΔE_1 (kJ mol^{-1})	−19.52	−19.01	−19.20	−19.29

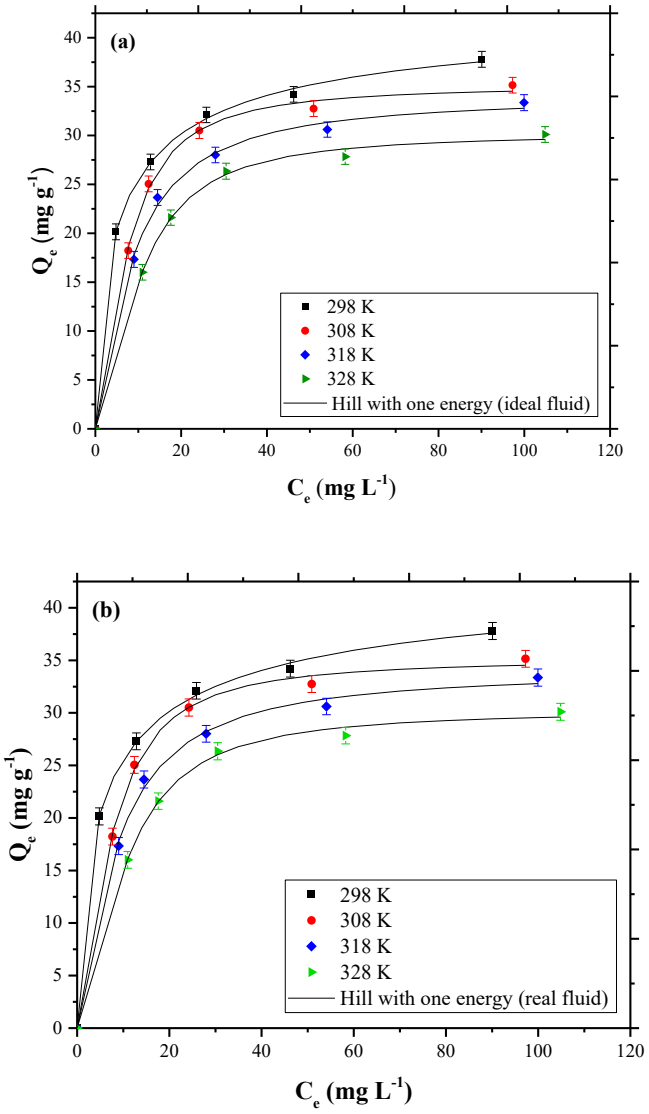

Fig. 2. GLY adsorption isotherms on MWCNT/MPNs-Fe (T = 298 to 328 K and pH 4) fitted to models (a) M1 and (b) M3.

tends to be the most correct. From the point of view of mathematical modeling, the simpler the model with the best fit, the more adequate is the interpretation of the process, since, from more elaborate models, it is possible to over-parameterize, that is, to add excess parameters without incurring improvement of description, and degrees of freedom may be lost in statistical analyses.

The selection of the M1 model confirms the assumption that intermolecular interactions between pesticide molecules can be neglected. The parameters of the physical-statistical model selected (Table 4) were interpreted according to the steric (n, N_m, Q_{sat}, W) and energetic (ΔE) classification associated with the adsorption mechanism.

5.2. Interpretation of steric parameters of the Hill model with 1 energy for an ideal fluid

5.2.1. Number of adsorbed GLY molecules per adsorbent site (n)

The parameter n (dimensionless) can be used to describe the behavior of pesticide molecules in the aqueous solution (before adsorption) and also on the surface of the adsorbent (after adsorption) [15]. Specifically, n is a steric coefficient representing the number of molecules adsorbed per adsorbent site. It allows estimating the degree of aggregation of the GLY molecules and their geometric adsorption positions on the MWCNT/MPNs-Fe surface [52]. The value of n is an average number, whether an integer or not, and three conditions are permissible for this parameter. Geometrically, the position of adsorbate can be described according to the number of shared molecules per site [43]: if $n \leq 0.5$, the GLY can be anchored by more receptor sites, suggesting that the position of the molecule is parallel to the surface of the MWCNT/MPNs-Fe, which corresponds to multi-anchoring adsorption; if $0.5 < n < 1$, GLY molecule can be adsorbed via a parallel and non-parallel orientation at the same time, implies a mixed anchorage; and if $n \geq 1$, the position of the adsorbate is non-parallel or leaning, but a larger number of molecules can be anchored in the same receptor site, corresponding to a multimolecular process [67,68,69]. https://www-sciencedirect.ez47.periodicos.capes.gov.br/science/article/pii/S0378381215301278 - bib10 Although the position of the adsorbate is the same for the second and third cases, a different degree of aggregation can be attributed [18]. In this sense, concerning aggregation: if $n < 1$, the molecules do not present aggregation; if $n = 1$, the molecules have a particular case of monomer formation; and if $n > 1$, one can attribute an aggregation phenomenon having dimer (n = 2), trimer (n = 3), among others [18,43].

As described in Table 4, for the GLY–MWCNTs/MPNs-Fe system, the values of n ranged from 0.67 to 1.66, with $0.5 < n < 1$ to 298 K and $n \geq 1$ at temperatures 308, 318, and 328 K. Concerning case $0.5 < n < 1$ (0.67 to 298 K), the process was identified as of mixed geometry (parallel and non-parallel orientation) on the surface of the adsorbent, with the corresponding anchor number (n′) equal to 1.49, indicating the anchorage of the GLY molecules by only one of the receptor sites available in the material (MPNs-Fe or COOH groups), more precisely by the interaction of the herbicide molecules with the MPNs-Fe, as previously evaluated by Diel et al. [44]. This trend is because the raw MWCNTs, with only COOH functionalization, showed almost insignificant removal and adsorptive capacity percentages. This behavior indicated that, without surface modification, these materials are not potential adsorbents for GLY removal. Therefore, the adsorption on MWCNT/MNPs-Fe is justified by the modification via green synthesis with MPNs-Fe. With the increase in temperature, the active site responsible for the adsorption started to attract more GLY molecules, contributing to the change from a mixed anchoring to a multimolecular process ($n \geq 1$). In addition, it changed adsorption orientation definitely to non-parallel.

Fig. 3 illustrates the evolution of the effect of temperature on n. It can be observed that the increase in temperature led to an increase in the estimated parameter, which can be attributed to thermal agitation [67]. While at 298 K, the absence of aggregation was identified, since the number of molecules captured per site is smaller ($n < 1$), generating activation energy that contributed to the phenomenon of aggregation, at higher temperatures, there was a degree of aggregation varying from a monomer ($n \approx 1$) to a dimer ($n \approx 2$). That is, the degree of aggregation increased with temperature, showing that temperature governs the aggregation phenomenon and that the system was energetically activated in the aqueous solution (i.e., before adsorption) [61]. This trend also confirms the change in the orientation of GLY molecules in the adsorbent as an effect of thermal agitation [31,43,60]. Therefore, the reduction of n from 328 to 298 K is commonly explained by breaking bonds of

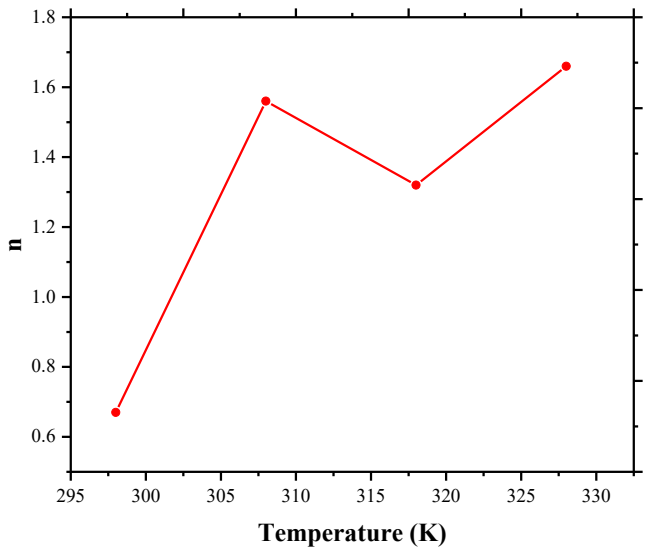

Fig. 3. Effect of temperature on parameter n of model M1.

GLY molecules in an aqueous solution.

5.2.2. Density of receptor sites (N_m)

The density of receptor sites (N_m, mg g^{-1}) is a steric parameter associated with the adsorbent sites effectively occupied during adsorption when saturation is reached, representing the number of sites capable of attracting adsorbate molecules in a given mass of the adsorbent [27,50]. According to Sellaoui et al. [51], the higher the N_m value, the greater the effectiveness of the adsorbent. Thus, in general, interpreting the number of molecules per site allows you to assess receptor sites' density easily.

The effect of temperature on the N_m parameter is shown in Fig. 4. Based on what was illustrated, N_m decreased as a function of temperature rise, pointing to an inverse trend to that reported for the n parameter. As n increased with increasing temperature, the corresponding density decreased, indicating that when the number of molecules per site is minimal, the density of the receptor site is maximum, reducing the adsorption sites occupied when saturation is reached. According to Sellaoui et al. [42,43,60], this reduction in N_m is related to the increase in the number of GLY molecules anchored per site and the degree of aggregation. Alyousef et al. [70], Hanafy et al. [61], and Sellaoui et al. [51] mention that the phenomenon of aggregation controlled the evolution of N_m, causing steric hindrance by hindering access to active sites on the adsorbent, since when the number of molecules per site increases, the space available for adsorption on the surface of the adsorbent tends to be reduced. This trend indicates that, at lower temperatures (298 K with $0.5 < n < 1$), the number of molecules captured per site was smaller compared to other temperatures, increasing the space available on the surface of the adsorbent and, consequently, the density of the receptor site was higher at this temperature.

5.2.3. Saturation adsorption capacity (Q_{sat})

The saturation adsorption capacity (Q_{sat}, mg g^{-1}) is a steric parameter that represents the amount of adsorbate adsorbed when the process reaches equilibrium and reaches the saturation state. In the physical-statistics formalism, the expression of Q_{sat} for the M1 model depends on the values above n and N_m, as pointed out in Equation (19). Fig. 5 reports the evolution of this parameter as a function of temperature for the investigated system.

According to Fig. 5, it can be identified that Q_{sat} decreased with increasing temperature (from 298 to 328 K), suggesting that GLY adsorption on MWCNT/MPNs-Fe is an exothermic phenomenon, favored at low temperatures. This behavior coincides with the thermodynamic calculations presented by Diel et al. [44] for that system, and a possible steric interpretation can be provided. Mathematically speaking, the product of the parameters n and N_m explains the decrease in Q_{sat} with temperature. In the case of n, the values increased as a function of temperature, but for N_m, the values were inversely proportional to temperature. Thus, it can be inferred that the density of receptor sites contributed more than the number of molecules per site to the behavior of Q_{sat} concerning temperature. Thus, Zhang et al. [52] point out that the pesticide adsorption mechanism is governed by the steric parameter N_m. According to Bouaziz et al. [48], this behavior is also due to the thermal agitation of the molecules during adsorption on the material's active sites. In conclusion, MWCNT/MPNs-Fe adsorbent should be used at lower temperatures to obtain adequate removal performance to treat water contaminated with GLY.

5.3. Interpretation of energy parameters of the Hill model with 1 energy for an ideal fluid

5.3.1. Adsorption energy (ΔE)

The adsorption energy (ΔE, kJ mol^{-1}) is an energy parameter that

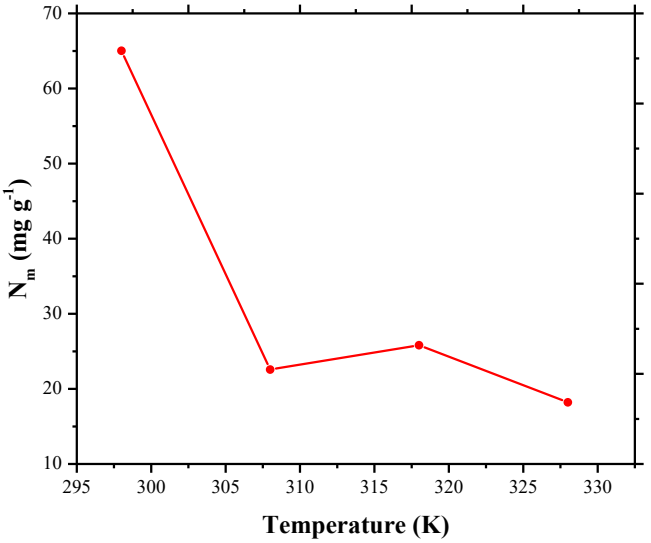

Fig. 4. Effect of temperature on the N_m parameter of the M1 model.

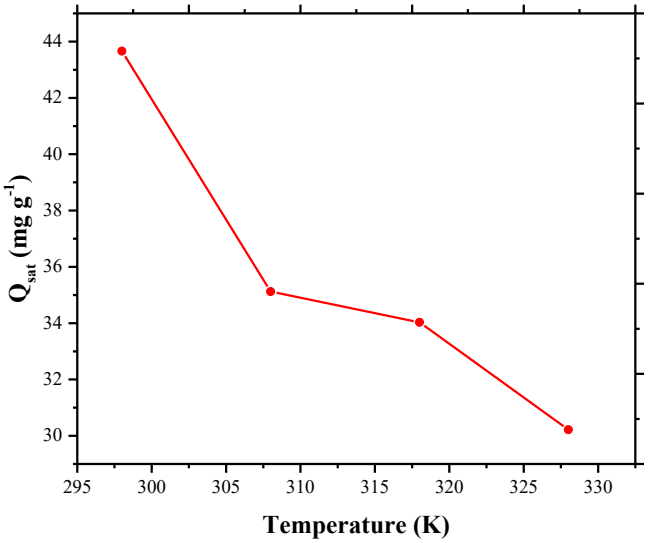

Fig. 5. Effect of temperature on the Q_{sat} parameter of model M1.

describes the interaction mechanisms involved between the adsorbate molecules and the functionalized surface of the adsorbent [52]. It can encompass the entire evolution of the model's steric parameters with temperature [18]. According to the expression in Equation 20, ΔE is dependent on the concentration at half-saturation obtained by fitting the data. Regarding the temperature effect, Fig. 6 shows the evolution of ΔE.

According to Fig. 6, a slight reduction in energy can be verified as a function of increasing temperature, remaining practically constant under the conditions studied. This observation suggests a negligible effect of temperature on adsorption energy [15]. Therefore, this parameter did not play the main role in the pesticide GLY removal mechanism in the investigated system. Regarding the magnitude of the values (Table 4), the estimated adsorption energies were<30 kJ mol^{-1}, reflecting that it is a process based on physisorption, characterized by electrostatic interactions, Van der Waals, or hydrogen bonds [15,42,43,46,61,62]. Therefore, the estimated values must be compared with the specific adsorption energies classified in the literature to identify the type of interaction. As for this classification, the system can be characterized from an energy point of view by applying the Conductor Type Screening Model for Real Solvents (COSMO-RS) [47] to estimate these specific interaction energies involved in pesticide adsorption on modified MWCNTs. Negative values corroborated with adsorption of an exothermic nature. Carrying out an interaction modeling in the *Multiwfn* software between the GLY molecule and the adsorbent, using as a parameter the electronegativity and the volume of the atoms involved, it was observed that hydrogen bonds could occur between the COOH functional group present in the adsorbent and the groups NH and COOH from GLY. Electrostatic interactions recognize the GLY COOH groups as negative points that interact directly with the positive Fe present in the material. Therefore, the interactions are weak and reversible adsorption is likely to occur, which allows exploring a desorption process for regeneration of the adsorbent [31], as proposed by Diel et al. [44].

6. Conclusions

The application of models based on the formalism of statistical physics presented new interpretations at the molecular level on the adsorption of GLY in modified carbon nanotubes via green synthesis (MWCNT/MPNs-Fe). According to the statistical indicators and the physical meaning of the parameters obtained, the Hill model with 1 energy and ideal fluid approach (M1) could predict the adsorption isotherms with greater precision than the other tested models. From the selection of the best fit model and the evaluation of the respective steric and energetic parameters, the main conclusions were: (I) under ideal conditions, the intermolecular interactions between the GLY molecules can be neglected; (II) the adsorption of GLY occurs through the formation of a monolayer, and the interactions of the pesticide with MWCNT/MPNs-Fe are characterized by only one energy; (III) the adsorption of GLY happens only in one of the two adsorption sites available in modified MWCNTs (MPNs-Fe or COOH), more precisely by the interaction of the pesticide molecules with the MPNs-Fe; (IV) the increase in temperature led to the increase of the n parameter, contributing to the change from process with mixed geometry ($0.5 < n < 1$) to multimolecular and non-parallel geometry ($n \geq 1$), in addition to influencing in the degree of aggregation of molecules, identifying that temperature governs the phenomenon of aggregation; (V) as n increased with increasing temperature, the corresponding density decreased, this reduction in Nm being related to the increase in the number of GLY molecules anchored per site and to the degree of aggregation of these molecules; (VI) from the product of the parameters n and N_m, which showed distinct trends as a function of temperature, it can be inferred that the density of receptor sites contributed more than the number of molecules per site to the behavior of Qsat in relation to temperature, indicating that the pesticide adsorption mechanism is governed by the steric parameter Nm; (VII) the combination of the above parameters and the magnitude of ΔE indicated that it is an exothermic process involving a physisorption mechanism, making it possible to explore a desorption process for regeneration of the adsorbent. Therefore, the insights indicate that the MWCNT/MPNs-Fe adsorbent favored pesticide adsorption by interacting molecules with the impregnated MPNs-Fe via green synthesis and the ideal application condition to obtain an adequate removal performance for the treatment GLY-contaminated water occurs at low temperatures.

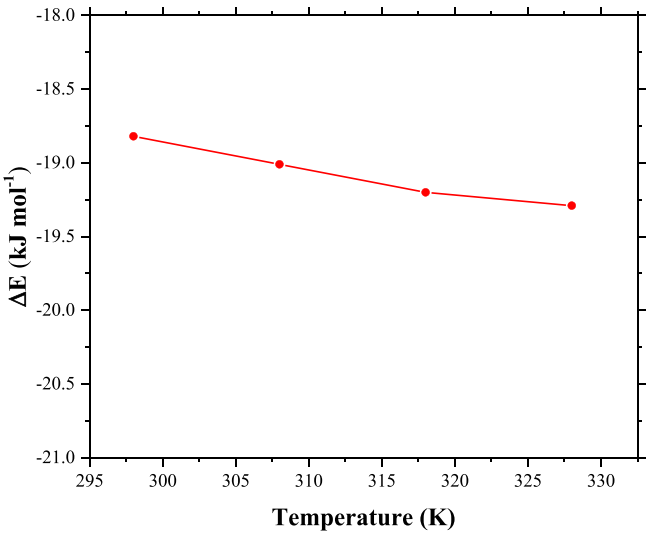

Fig. 6. Effect of temperature on the ΔE parameter of model M1.

Declaration of Competing Interest

The authors declare that they have no known competing financial interests or personal relationships that could have appeared to influence the work reported in this paper.

Appendix A. Supplementary data

Supplementary data to this article can be found online at https://doi.org/10.1016/j.cej.2021.134095.

References

[1] B. Fernández-Reyes, K. Ortiz-Martínez, J.A. Lasalde-Ramírez, A.J. Hernández-Maldonado, Engineered adsorbents for the removal of contaminants of emerging concern from water, in: Contaminants of Emerging Concern in Water and Wastewater, Elsevier Inc., 2020, pp. 3–45, https://doi.org/10.1016/B978-0-12-813561-7.00001-8.
[2] J. Scaria, A. Gopinath, P.V. Nidheesh, A versatile strategy to eliminate emerging contaminants from the aqueous environment: Heterogeneous Fenton process, J. Clean. Prod. 278 (2021) 124014, https://doi.org/10.1016/j.jclepro.2020.124014.
[3] World Health Organization (WHO), 1994. Environmental Health Criteria 159: Glyphosate [WWW Document].
[4] S. Fiorilli, L. Rivoira, G. Calì, M. Appendini, M. Concetta, M. Coïsson, B. Onida, Applied Surface Science Iron oxide inside SBA-15 modified with amino groups as reusable adsorbent for highly efficient removal of glyphosate from water, Appl. Surf. Sci. 411 (2017) 457–465, https://doi.org/10.1016/j.apsusc.2017.03.206.
[5] R. Mesnage, M.N. Antoniou, Facts and Fallacies in the Debate on Glyphosate Toxicity, Front. Public Heal. 5 (2017) 1–7, https://doi.org/10.3389/fpubh.2017.00316.
[6] Y. Yang, Q. Deng, W. Yan, C. Jing, Y. Zhang, Comparative study of glyphosate removal on goethite and magnetite: Adsorption and photo-degradation, Chem. Eng. J. 352 (2018) 581–589, https://doi.org/10.1016/j.cej.2018.07.058.
[7] N.U. Yamaguchi, R. Bergamasco, S. Hamoudi, Magnetic MnFe2O4–graphene hybrid composite for efficient removal of glyphosate from water, Chem. Eng. J. 295 (2016) 391–402, https://doi.org/10.1016/j.cej.2016.03.051.
[8] Z. Liu, M. Zhu, P. Yu, Y. Xu, X. Zhao, Pretreatment of membrane separation of glyphosate mother liquor using a precipitation method, Desalination 313 (2013) 140–144, https://doi.org/10.1016/j.desal.2012.12.011.
[9] H. Rubí-Juárez, S. Cotillas, C. Sáez, P. Cañizares, C. Barrera-Díaz, M.A. Rodrigo, Use of conductive diamond photo-electrochemical oxidation for the removal of

pesticide glyphosate, Sep. Purif. Technol. 167 (2016) 127–135, https://doi.org/10.1016/j.seppur.2016.04.048.
[10] S. Chen, Y. Liu, Study on the photocatalytic degradation of glyphosate by TiO2 photocatalyst, Chemosphere 67 (5) (2007) 1010–1017, https://doi.org/10.1016/j.chemosphere.2006.10.054.
[11] A. Serra-Clusellas, L. De Angelis, M. Beltramo, M. Bava, J. De Frankenberg, J. Vigliarolo, N. Di Giovanni, J.D. Stripeikis, J.A. Rengifo-Herrera, M.M. Fidalgo De Cortalezzi, Glyphosate and AMPA removal from water by solar induced processes using low Fe(III) or Fe(II) concentrations, Environ. Sci. Water Res. Technol. 5 (2019) 1932–1942, https://doi.org/10.1039/c9ew00442d.
[12] T. Zheng, Y. Sun, Y. Lin, N. Wang, P. Wang, Study on preparation of microwave absorbing MnOx/Al2O3 adsorbent and degradation of adsorbed glyphosate in MW-UV system, Chem. Eng. J. 298 (2016) 68–74, https://doi.org/10.1016/j.cej.2016.03.143.
[13] M.R. Assalin, S.G. De Moraes, S.C.N. Queiroz, V.L. Ferracini, N. Duran, Studies on degradation of glyphosate by several oxidative chemical processes: Ozonation, photolysis and heterogeneous photocatalysis. J. Environ. Sci. Heal. - Part B Pestic, Food Contam. Agric. Wastes 45 (1) (2009) 89–94, https://doi.org/10.1080/03601230903404598.
[14] Z. Shamsollahi, A. Partovinia, Recent advances on pollutants removal by rice husk as a bio-based adsorbent: A critical review, J. Environ. Manage. 246 (2019) 314–323, https://doi.org/10.1016/j.jenvman.2019.05.145.
[15] X. Pang, L. Sellaoui, D. Franco, G.L. Dotto, J. Georgin, A. Bajahzar, H. Belmabrouk, A. Ben Lamine, A. Bonilla-Petriciolet, Z. Li, Adsorption of crystal violet on biomasses from pecan nutshell, para chestnut husk, araucaria bark and palm cactus: Experimental study and theoretical modeling via monolayer and double layer statistical physics models, Chem. Eng. J. 378 (2019) 122101, https://doi.org/10.1016/j.cej.2019.122101.
[16] P.V.S. Lins, D.C. Henrique, A.H. Ide, J.L.d.S. Duarte, G.L. Dotto, A. Yazidi, L. Sellaoui, A. Erto, C.L. Zanta, L. Meili, Adsorption of a non-steroidal anti-inflammatory drug onto MgAl/LDH-activated carbon composite – Experimental investigation and statistical physics modeling, Colloids Surfaces A Physicochem. Eng. Asp. 586 (2020) 124217, https://doi.org/10.1016/j.colsurfa.2019.124217.
[17] C.R. Zhou, G.P. Li, D.G. Jiang, Study on behavior of alkalescent fiber FFA-1 adsorbing glyphosate from production wastewater of glyphosate, Fluid Phase Equilib. 362 (2014) 69–73.
[18] G.L. Dotto, E. Chaves, Y. Benguerba, É. Cláudio, A. Ben, A. Erto, New insights into the adsorption of crystal violet dye on functionalized multi-walled carbon nanotubes : Experiments, statistical physics and COSMO – RS models application 248 (2017) 890–897, https://doi.org/10.1016/j.molliq.2017.10.124.
[19] R.T.A. Carneiro, T.B. Taketa, R.J. Gomes Neto, J.L. Oliveira, E.V.R. Campos, M.A. D. Moraes, C.M.G. Silva, M.M. Beppu, L.F. Fraceto, Removal of glyphosate herbicide from water using biopolymer membranes, J. Environ. Manage. 151 (2015) 353–360, https://doi.org/10.1016/j.jenvman.2015.01.005.
[20] F. Chen, C. Zhou, G.-P. Li, F.-F. Peng, Thermodynamics and kinetics of glyphosate adsorption on resin D301, Arab. J. Chem. 9 (2016) S1665–S1669, https://doi.org/10.1016/j.arabjc.2012.04.014.
[21] I. Herath, P. Kumarathilaka, M.I. Al-Wabel, A. Abduljabbar, M. Ahmad, A.R. A. Usman, M. Vithanage, Mechanistic modeling of glyphosate interaction with rice husk derived engineered biochar, Microporous Mesoporous Mater. 225 (2016) 280–288, https://doi.org/10.1016/j.micromeso.2016.01.017.
[22] P. Marin, R. Bergamasco, A.N. Módenes, P.R. Paraiso, S. Hamoudi, Synthesis and characterization of graphene oxide functionalized with MnFe2O4 and supported on activated carbon for glyphosate adsorption in fixed bed column, Process Saf. Environ. Prot. 123 (2019) 59–71, https://doi.org/10.1016/j.psep.2018.12.027.
[23] S.S. Mayakaduwa, P. Kumarathilaka, I. Herath, M. Ahmad, M. Al-Wabel, Y.S. Ok, A. Usman, A. Abduljabbar, M. Vithanage, Equilibrium and kinetic mechanisms of woody biochar on aqueous glyphosate removal, Chemosphere 144 (2016) 2516–2521, https://doi.org/10.1016/j.chemosphere.2015.07.080.
[24] L. Ramrakhiani, S. Ghosh, A.K. Mandal, S. Majumdar, Utilization of multi-metal laden spent biosorbent for removal of glyphosate herbicide from aqueous solution and its mechanism elucidation, Chem. Eng. J. 361 (2019) 1063–1077.
[25] S. Zavareh, Z. Farrokhzad, F. Darvishi, Modification of zeolite 4A for use as an adsorbent for glyphosate and as an antibacterial agent for water, Ecotoxicol. Environ. Saf. 155 (2018) 1–8, https://doi.org/10.1016/j.ecoenv.2018.02.043.
[26] L. Samuel, R. Wang, G. Dubois, R. Allen, R. Wojtecki, Y.-H. La, Amine-functionalized, multi-arm star polymers: A novel platform for removing glyphosate from aqueous media, Chemosphere 169 (2017) 437–442, https://doi.org/10.1016/j.chemosphere.2016.11.049.
[27] F.K. Rodrigues, N.P.G. Salau, G.L. Dotto, New insights about reactive red 141 adsorption onto multi–walled carbon nanotubes using statistical physics coupled with Van der Waals equation, Sep. Purif. Technol. 224 (2019) 290–294, https://doi.org/10.1016/j.seppur.2019.05.042.
[28] T. Rasheed, M. Adeel, F. Nabeel, M. Bilal, H.M.N. Iqbal, TiO2/SiO2 decorated carbon nanostructured materials as a multifunctional platform for emerging pollutants removal, Sci. Total Environ. 688 (2019) 299–311, https://doi.org/10.1016/j.scitotenv.2019.06.200.
[29] C. Parlak, Ö. Alver, Adsorption of ibuprofen on silicon decorated fullerenes and single walled carbon nanotubes: A comparative DFT study, J. Mol. Struct. 1184 (2019) 110–113, https://doi.org/10.1016/j.molstruc.2019.02.023.
[30] A. Avcı, İ. İnci, N. Baylan, Adsorption of ciprofloxacin hydrochloride on multiwall carbon nanotube, J. Mol. Struct. 1206 (2020) 127711, https://doi.org/10.1016/j.molstruc.2020.127711.
[31] Z. Li, L. Sellaoui, D. Franco, M.S. Netto, J. Georgin, G.L. Dotto, A. Bajahzar, H. Belmabrouk, A. Bonilla-Petriciolet, Q. Li, Adsorption of hazardous dyes on functionalized multiwalled carbon nanotubes in single and binary systems: Experimental study and physicochemical interpretation of the adsorption mechanism, Chem. Eng. J. 389 (2020) 124467, https://doi.org/10.1016/j.cej.2020.124467.
[32] L.D.T. Prola, F.M. Machado, C.P. Bergmann, F.E. de Souza, C.R. Gally, E.C. Lima, M.A. Adebayo, S.L.P. Dias, T. Calvete, Adsorption of Direct Blue 53 dye from aqueous solutions by multi-walled carbon nanotubes and activated carbon, J. Environ. Manage. 130 (2013) 166–175, https://doi.org/10.1016/j.jenvman.2013.09.003.
[33] Y.-H. Li, S. Wang, Z. Luan, J. Ding, C. Xu, D. Wu, Adsorption of cadmium(II) from aqueous solution by surface oxidized carbon nanotubes, Carbon N. Y. 41 (5) (2003) 1057–1062, https://doi.org/10.1016/S0008-6223(02)00440-2.
[34] Y.-H. Li, S. Wang, J. Wei, X. Zhang, C. Xu, Z. Luan, D. Wu, B. Wei, Lead adsorption on carbon nanotubes, Chem. Phys. Lett. 357 (3-4) (2002) 263–266.
[35] Ö. Çelebican, İ. İnci, N. Baylan, Modeling and optimization of formic acid adsorption by multiwall carbon nanotube using response surface methodology, J. Mol. Struct. 1203 (2020) 127312, https://doi.org/10.1016/j.molstruc.2019.127312.
[36] D. Lin, B. Xing, Adsorption of Phenolic Compounds by Carbon Nanotubes: Role of Aromaticity and Substitution of Hydroxyl Groups, Environ. Sci. Technol. 42 (19) (2008) 7254–7259, https://doi.org/10.1021/es801297u.
[37] Z. Hu, H. Xie, Q. Wang, S. Chen, Adsorption and diffusion of sulfur dioxide and nitrogen in single-wall carbon nanotubes, J. Mol. Graph. Model. 88 (2019) 62–70, https://doi.org/10.1016/j.jmgm.2019.01.003.
[38] S.S. Fiyadh, M.A. AlSaadi, W.Z. Jaafar, M.K. AlOmar, S.S. Fayaed, N.S. Mohd, L. S. Hin, A. El-Shafie, Review on heavy metal adsorption processes by carbon nanotubes, J. Clean. Prod. 230 (2019) 783–793, https://doi.org/10.1016/j.jclepro.2019.05.154.
[39] J.C. Diel, D.S.P. Franco, A.V. Igansi, T.R.S. Cadaval, H.A. Pereira, I.D.S. Nunes, C. W. Basso, M.d.C.M. Alves, J. Morais, D. Pinto, G.L. Dotto, Green synthesis of carbon nanotubes impregnated with metallic nanoparticles: Characterization and application in glyphosate adsorption, Chemosphere 283 (2021) 131193, https://doi.org/10.1016/j.chemosphere.2021.131193.
[40] Z. Li, L. Sellaoui, G.L. Dotto, A.B. Lamine, A. Bonilla-Petriciolet, H. Hanafy, H. Belmabrouk, M.S. Netto, A. Erto, Interpretation of the adsorption mechanism of Reactive Black 5 and Ponceau 4R dyes on chitosan/polyamide nanofibers via advanced statistical physics model, J. Mol. Liq. 285 (2019) 165–170, https://doi.org/10.1016/j.molliq.2019.04.091.
[41] D.S.P. Franco, J.S. Piccin, E.C. Lima, G.L. Dotto, Interpretations about methylene blue adsorption by surface modified chitin using the statistical physics treatment, Adsorption 21 (8) (2015) 557–564, https://doi.org/10.1007/s10450-015-9699-z.
[42] L. Sellaoui, É.C. Lima, G.L. Dotto, S.L.P. Dias, A. Ben Lamine, Physicochemical modeling of reactive violet 5 dye adsorption on home-made cocoa shell and commercial activated carbons using the statistical physics theory, Results Phys. 7 (2017) 233–237, https://doi.org/10.1016/j.rinp.2016.12.014.
[43] L. Sellaoui, N. Mechi, É.C. Lima, G.L. Dotto, A. Ben Lamine, Adsorption of diclofenac and nimesulide on activated carbon: Statistical physics modeling and effect of adsorbate size, J. Phys. Chem. Solids 109 (2017) 117–123, https://doi.org/10.1016/j.jpcs.2017.05.019.
[44] J.C. Diel, D.S.P. Franco, I.D.S. Nunes, H.A. Pereira, K.S. Moreira, T.A. de L. Burgo, E.L. Foletto, G.L. Dotto, Carbon nanotubes impregnated with metallic nanoparticles and their application as an adsorbent for the glyphosate removal in an aqueous matrix, J. Environ. Chem. Eng. 9 (2) (2021) 105178, https://doi.org/10.1016/j.jece:2021.105178.
[45] B. Bhaskara, P. Nagaraja, Direct Sensitive Spectrophotometric Determination of Glyphosate by Using Ninhydrin as a Chromogenic Reagent in Formulations and Environmental Water Samples, Helv. Chim. Acta 89 (11) (2006) 2686–2693, https://doi.org/10.1002/(ISSN)1522-267510.1002/hlca.v89:1110.1002/hlca.200690240.
[46] L. Sellaoui, S. Knani, A. Erto, M.A. Hachicha, A. Ben Lamine, Equilibrium isotherm simulation of tetrachlorethylene on activated carbon using the double layer model with two energies: Steric and energetic interpretations, Fluid Phase Equilib. 408 (2016) 259–264, https://doi.org/10.1016/j.fluid.2015.09.022.
[47] K.H. Toumi, Y. Benguerba, A. Erto, G.L. Dotto, M. Khalfaoui, C. Tiar, S. Nacef, A. Amrane, Molecular modeling of cationic dyes adsorption on agricultural Algerian olive cake waste, J. Mol. Liq. 264 (2018) 127–133, https://doi.org/10.1016/j.molliq.2018.05.045.
[48] N. Bouaziz, M. Ben, F. Aouaini, A. Ben, Investigation of hydrogen adsorption on zeolites A, X and Y using statistical physics formalism, Mater. Chem. Phys. 225 (2019) 111–121, https://doi.org/10.1016/j.matchemphys.2018.12.024.
[49] F. Ayachi, E.C. Lima, A. Sakly, H. Mejri, A. Ben, Modeling of adsorption isotherms of reactive red RR-120 on spirulina platensis by statistical physics formalism involving interaction effect between adsorbate molecules, Prog. Biophys. Mol. Biol. 141 (2019) 47–59, https://doi.org/10.1016/j.pbiomolbio.2018.07.004.
[50] A. Yazidi, L. Sellaoui, G.L. Dotto, A. Bonilla-Petriciolet, A.C. Fröhlich, A.B. Lamine, Monolayer and multilayer adsorption of pharmaceuticals on activated carbon: Application of advanced statistical physics models, J. Mol. Liq. 283 (2019) 276–286, https://doi.org/10.1016/j.molliq.2019.03.101.
[51] L. Sellaoui, H. Guedidi, S. Knani, L. Reinert, L. Duclaux, A. Ben Lamine, Application of statistical physics formalism to the modeling of adsorption isotherms of ibuprofen on activated carbon, Fluid Phase Equilib. 387 (2015) 103–110, https://doi.org/10.1016/j.fluid.2014.12.018.
[52] L. Zhang, L. Sellaoui, D. Franco, G.L. Dotto, A. Bajahzar, H. Belmabrouk, A. Bonilla-Petriciolet, M.L.S. Oliveira, Z. Li, Adsorption of dyes brilliant blue, sunset yellow and tartrazine from aqueous solution on chitosan: Analytical interpretation via multilayer statistical physics model, Chem. Eng. J. 382 (2020) 122952, https://doi.org/10.1016/j.cej.2019.122952.

[53] E. Mezura-Montes, C.A. Coello Coello, Constraint-handling in nature-inspired numerical optimization: Past, present and future, Swarm Evol. Comput. 1 (4) (2011) 173–194, https://doi.org/10.1016/j.swevo.2011.10.001.
[54] J. Kennedy, R. Eberhart, Particle Swarm Optimisation. Stud, Comput. Intell. 927 (1995) 1942–1948, https://doi.org/10.1007/978-3-030-61111-8_2.
[55] K. Levenberg, A method for the solution of certain non-linear problems in least squares, Q. Appl. Math. 2 (2) (1944) 164–168, https://doi.org/10.1090/qam/1944-02-0210.1090/qam/10666.
[56] D.W. Marquardt, An Algorithm for Least-Squares Estimation of Nonlinear Parameters, J. Soc. Ind. Appl. Math. 11 (2) (1963) 431–441, https://doi.org/10.1137/0111030.
[57] J.J. Moré, The Leveberg-Marquardt Algorithm: Implementation and Theory, Numer. Anal. (1977) 105–116.
[58] C.L. da Silveira, M.A. Mazutti, N.PG. Salau, Solid-state fermentation process model reparametrization procedure for parameters estimation using particle swarm optimization, J. of Chem. Tech. and Biotech. 91 (3) (2016) 762–768, https://doi.org/10.1002/jctb.2016.91.issue-310.1002/jctb.4642.
[59] C.L. Silveira, A.C. Galvão, W.S. Robazza, J.V.T. Feyh, Modeling and parameters estimation for the solubility calculations of nicotinamide using UNIFAC and COSMO-based models, Fluid Phase Equilibria 535 (2021) 112970, https://doi.org/10.1016/j.fluid.2021.112970.
[60] L. Sellaoui, B.B. Saha, S. Wjihi, A.B. Lamine, Physicochemical parameters interpretation for adsorption equilibrium of ethanol on metal organic framework: Application of the multilayer model with saturation, J. Mol. Liq. 233 (2017) 537–542, https://doi.org/10.1016/j.molliq.2016.07.017.
[61] H. Hanafy, L. Sellaoui, P.S. Thue, E.C. Lima, G.L. Dotto, T. Alharbi, H. Belmabrouk, A. Bonilla-Petriciolet, A.B. Lamine, Statistical physics modeling and interpretation of the adsorption of dye remazol black B on natural and carbonized biomasses, J. Mol. Liq. 299 (2020) 112099, https://doi.org/10.1016/j.molliq.2019.112099.
[62] M. Khalfaoui, A. Nakhli, S. Knani, H.V. Baouab, A.B. Lamine, On the Statistical Physics Modeling of Dye Adsorption onto Anionized Nylon, Consequent New Interpretations 125 (2012) 1091–1102, https://doi.org/10.1002/app.
[63] O.P.d. Amarante Junior, T.C.R.D. Santos, N.M. Brito, M.L. Ribeiro, Glifosato: propriedades, toxicidade, usos e legislação, Quim. Nova 25 (4) (2002) 589–593.
[64] Bonilla-Petriciolet, A., Mendoza-Castillo, D.I., Dotto, G.L., Duran-Valle, C.J., 2019. Adsorption in Water Treatment. Chem. Mol. Sci. Chem. Eng. 1–19.
[65] Bonilla-Petriciolet, A., Mendoza-Castillo, D.I., Reynel-Ávila, H.E., 2017. Adsorption processes for water treatment and purification, Springer. ed, Adsorption Processes for Water Treatment and Purification. México. https://doi.org/10.1007/978-3-319-58136-1.
[66] S. Knani, M. Khalfaoui, M.A. Hachicha, A. Ben Lamine, M. Mathlouthi, Modelling of water vapour adsorption on foods products by a statistical physics treatment using the grand canonical ensemble, Food Chem. 132 (4) (2012) 1686–1692, https://doi.org/10.1016/j.foodchem.2011.11.065.
[67] M.B. Manaa, N. Wazzan, A.B. Lamine, Physico-chemical interpretations of the adsorption isotherms of D-π-A sensitizers with pyridyl group on TiO2 for dye sensitized solar cells using statistical physics and density functional theory, J. Mat. Reser. Tech. 15 (2021) 369–383, https://doi.org/10.1016/j.jmrt.2021.08.017.
[68] H.A. Al-Yousef, B.M. Alotaibi, F. Aouaini, L. Sellaoui, A. Bonilla-Petriciolet, Adsorption of ibuprofen on cocoa shell biomass-based adsorbents: Interpretation of the adsorption equilibriumvia statistical physics theory, J. Mol. Liq. 331 (2021) 115697, https://doi.org/10.1016/j.molliq.2021.115697.
[69] M.S. Shamsudin, S.F. Azha, L. Sellaoui, M. Badawi, A. Bonilla-Petriciolet, S. Ismail, Performance and interactions of diclofenac adsorption using Alginate/ Carbon-based Films: Experimental investigation and statistical physics modelling, Chem. Eng. J. 428 (2022) 131929, https://doi.org/10.1016/j.cej.2021.131929.
[70] H. Alyousef, M. Ben, F. Aouaini, Statistical physics modeling of water vapor adsorption isotherm into kernels of dates : Experiments, microscopic interpretation and thermodynamic functions evaluation, Arab. J. Chem. 13 (2020) 4691–4702, https://doi.org/10.1016/j.arabjc.2019.11.004.